Ion Beam Divergence Characteristics of Three-Grid Accelerator Systems

Graeme Aston*and Harold R. Kaufman†
Colorado State University, Fort Collins, Colo.

A comprehensive experimental investigation of the geometrical and operating conditions which affect most strongly the ion beam divergence of three-grid accelerator systems is presented. Three-grid accelerator systems are shown to offer significant improvements in ion beam focusing over two-grid accelerator systems. These improvements are greatest for low net-to-total accelerating voltage ratios and small screen-to-accelerator grid separation ratios (i.e., high perveance grid sets). Ion beam focusing gains are negligible at a net-to-total accelerating voltage ratio near unity. Low decelerator grid impingement currents and low ion beam divergence angles require that the decelerator hole diameter be about 25% larger than the accelerator hole diameter, and also that the decelerator grid be spaced as close as is practically possible to the accelerator grid. The graphical results contained herein provide guidelines for the design of three-grid ion accelerator systems.

Nomenclature

d_a = accelerator hole diameter
d_d = decelerator hole diameter
d_s = screen hole diameter
f_D = ion beam divergence factor
J_B = beam current per hole
l_d = accelerator-to-decelerator grid separation
l_e = effective acceleration length[2,4]
l_g = screen-to-accelerator grid separation
R = net-to-total accelerating voltage ratio
t_a = accelerator grid thickness
t_d = decelerator grid thickness
t_s = screen grid thickness
V_D = discharge voltage
V_n = net accelerating voltage
V_T = total accelerating voltage
α = ion beam divergence angle

I. Introduction

THE addition of a third (decelerator) grid to a two-grid ion‡ accelerator system is known to reduce ion beam divergence from electron-bombardment thrusters.[1] The decelerator grid is maintained at, or close to, facility ground potential and positioned downstream of the accelerator grid. This fixes the neutralization surface at the decelerator grid potential, resulting in flatter equipotential surfaces between the neutralization plane and each accelerator grid hole than with a two-grid accelerator system. Flatter equipotential surfaces in the ion deceleration region cause less off-axis deflection of the emerging ions. This results in decreased ion beam divergence over that obtained by using a two-grid accelerator system.

The purpose of this study has been to determine those geometrical and operating conditions that affect most strongly the ion beam divergence of three-grid accelerator systems. Previous two-grid accelerator system studies have shown that ion beam divergence depends most strongly on normalized perveance per hole, screen-to-accelerator grid separation ratio, and net-to-total accelerating voltage ratio.[2] These parameters, along with the decelerator grid location and geometry, were the quantities investigated most thoroughly in this report.

II. Apparatus and Procedure

Figure 1 depicts a portion of a multiaperture three-grid accelerator system showing the coaxial hole geometry and ion beamlet formation. In the data presented hereafter the following parameters were kept at the values indicated unless specified otherwise: screen hole diameter $d_s = 2.06$ mm, screen grid thickness ratio $t_s/d_s = 0.185$, accelerator grid thickness ratio $t_a/d_s = 0.370$, decelerator grid thickness ratio $t_d/d_s = 0.370$, accelerator hole diameter ratio $d_a/d_s = 0.642$, decelerator hole diameter ratio $d_d/d_s = 0.827$, total accelerating voltage $V_T = 1100$ V and discharge voltage $V_D = 40$ V. The apparatus and procedure used for this study were identical to that used during a previous accelerator system investigation,[2] except for the addition of the decelerator grid. Briefly, a mildly divergent magnetic field 8-cm-diam electron-bombardment ion source was constructed and operated on argon propellant. Tungsten wire filaments were used as both the main and neutralizer cathode emitters. The screen, accelerator, and decelerator grids were made from thin flat sheet graphite. The grid aperture pattern comprised a 19-hole hexagonal array with a center-to-center hole spacing of 2.54 mm. Variable grid separation was accomplished by using various numbers of thin mica washers (0.254-mm thick). The assembled accelerator system was placed on a masked-down discharge chamber, which insured that the 1-cm^2 hexagonal hole array extracted ions from a near uniform plasma. While some grid warpage could occur during operation, the magnitude of this warpage should be small because the grids were made of carbon and the greatest distance between grid supports was less than 2 cm. Beam divergence measurements were accomplished using a movable probe rake, containing 20 individual Faraday ion current sensors, positioned at varying distances downstream of the accelerator system. The Faraday ion current sensors were screened and biased to reflect neutralization electrons and low energy charge exchange ions present in the beam plasma. The ion beam divergence angle α was defined as the truncated cone angle enclosing 95% of the total integrated beam current. The ion beam divergence factor f_D was defined as the ratio of the net axial thrust produced by

Presented as Paper 78-669 at the AIAA/DGLR 13th International Electric Propulsion Conference,San Diego,Calif., April 25-27, 1978; submitted May 15, 1978, revision received Sept. 19, 1978.

Index category: Electric and Advanced Space Propulsion.

*Research Assistant, Dept. of Physics. Student Member AIAA.

†Professor, Depts. of Physics and Mechanical Engineering. Associate Fellow AIAA.

‡Since this work deals only with singly charged positive ions, the term "ion" is used with the exclusive meaning "singly charged positive ion."

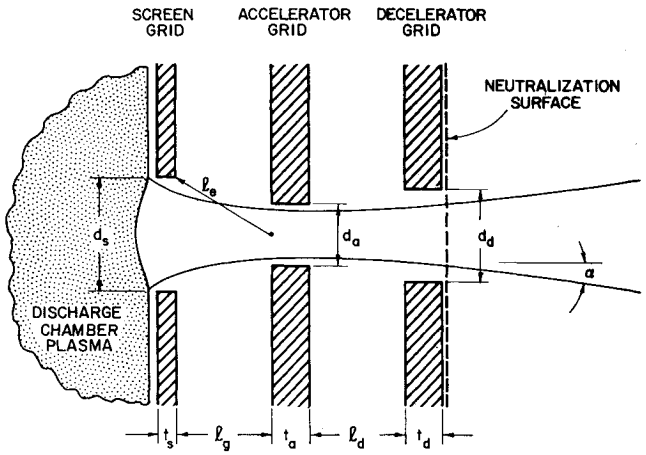

Fig. 1 Three-grid accelerator system.

the divergent ion beam to the thrust produced if the ion beam were perfectly collimated. A more complete discussion of the parameters α and f_D is contained in Ref. 2. Each grid set geometry investigated was operated over a range of increasing cathode emission levels to the maximum beam current obtainable from that grid set. The approach to this maximum was usually characterized by a rapid increase in either accelerator or decelerator grid impingement current and a negligible beam current increase. Ion beam divergence data were obtained at selected beam currents leading up to this maximum. All source operation was conducted in a 30-cm pyrex bell jar. Average bell jar pressure was 1×10^{-4} Torr.

III. Results and Discussion

The parameter, normalized perveance per hole,[2] is used to correlate the beam current variations of each grid set geometry investigated. Normalized perveance per hole values are based on the argon propellant ion mass because argon was the test gas used. The results are applicable for other propellant atoms if the normalized perveance per hole values used herein are multiplied by the square root of the ratio of the atomic weight of argon to the atomic weight of the propellant to be used. The precision with which the ion beam divergence data were obtained is $\pm$ 0.5 deg for α and ± 0.001 for f_D. The absolute accuracy of the data is thought to be better than ± 1.0 deg for α and $\pm$ 0.002 for f_D. A tabular listing of all the experimental results obtained during this study has been presented previously.[3]

Ion Beam Divergence Angle

Figures 2 and 3 show the beam divergence characteristics of a high perveance grid set (small screen-to-accelerator grid separation ratio l_g/d_s) as the accelerator-to-decelerator grid separation ratio l_d/d_s and net-to-total accelerating voltage ratio R are varied over the range of interest. Either increasing the net-to-total accelerating voltage ratio or decreasing the accelerator-to-decelerator grid separation ratio is observed to decrease ion beam divergence. Ion beam divergence becomes less sensitive to changes in the accelerator-to-decelerator grid separation ratio as the net-to-total accelerating voltage ratio approaches unity (Fig. 3) or the accelerator-to-decelerator grid separation ratio approaches some value close to 0.1 (Fig. 2). Figure 2 also shows that decreasing the accelerator-to-decelerator grid separation ratio increases the maximum normalized perveance per hole; this permits a greater operating range near the minimum beam divergence angle. This effect becomes less pronounced at higher R values (Fig. 3). The beam divergence angle reductions at normalized perveance per hole values less than those corresponding to the maximum ion beam divergence angle, seen in Figs. 2 and 3, result from direct ion impingement upon the decelerator grid. This reduction in divergence angle appears to occur because

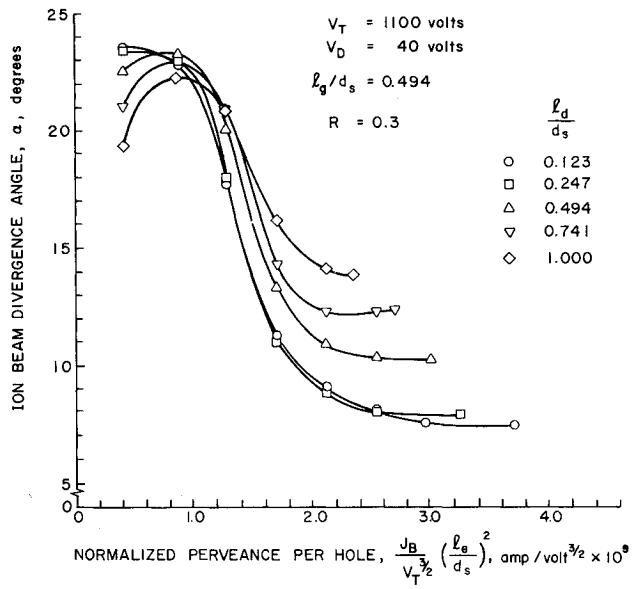

Fig. 2 Effect of l_d/d_s on ion beam divergence (small l_g/d_s and small R).

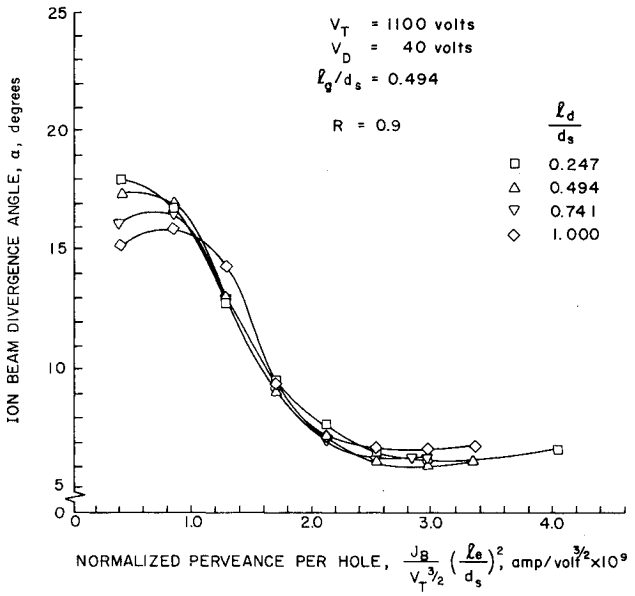

Fig. 3 Effect of l_d/d_s on ion beam divergence (small l_g/d_s and large R).

the beamlet ions impinging upon the decelerator grid at low normalized perveance per hole, or beam current, values are those which have the greatest off-axis velocity components. By intercepting these ions, the decelerator grid acts as a beamlet mask which reduces the beam divergence angle at low normalized perveance per hole values. Evidence of the high decelerator grid impingement currents at low normalized perveance per hole values is shown in Fig. 4. Here, accelerator and decelerator grid impingement currents, expressed as a percentage of beam current, are plotted against normalized perveance per hole for the extreme cases of accelerator-to-decelerator grid separation ratio presented in Fig. 2. Decelerator grid impingement current is observed to increase sharply with an increase in the accelerator-to-decelerator grid separation ratio (Fig. 4a). Figure 4b shows that increasing the net-to-total accelerating voltage ratio for a given grid set geometry reduces the decelerator grid impingement current.

Figure 5 shows the effect on ion beam divergence as l_d/d_s is varied for an extreme R value of 0.1. Although ion beam focusing is poor for both accelerator-to-decelerator grid

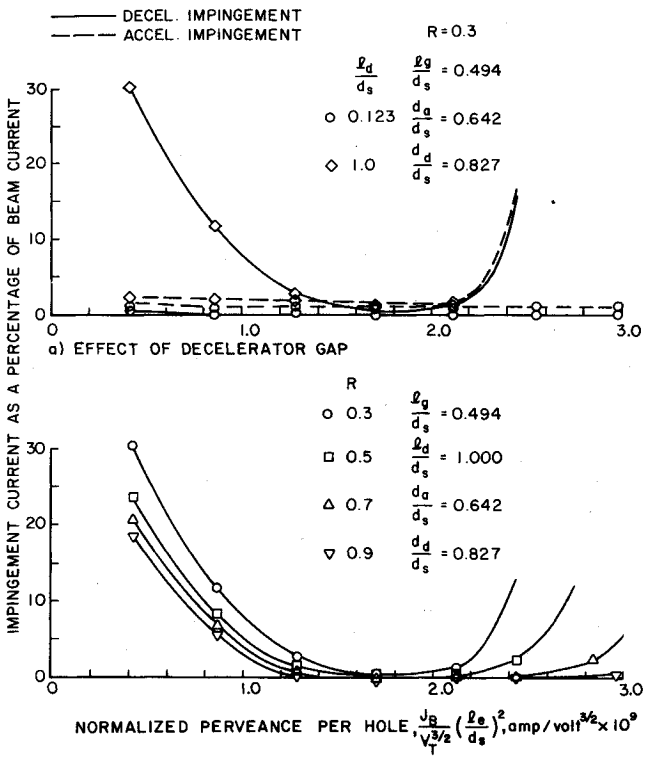

Fig. 4 Three-grid impingement current characteristics.

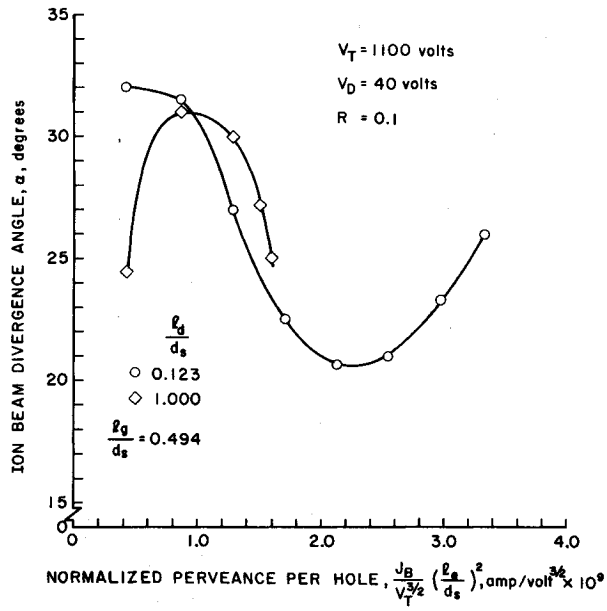

Fig. 5 Effect of l_d/d_s on ion beam divergence (small l_g/d_s and very small R).

separation ratios, the maximum perveance at $l_d/d_s = 1.000$ was considerably lower because of excessive decelerator grid impingement currents. These currents were never less than 200 μA (full scale on the meter) for all beam currents tested. For $l_d/d_s = 0.123$, on the other hand, these impingement currents were acceptably low. Other tests showed that increasing the total accelerating voltage V_T from 1100 to 1500 V at this extreme net-to-total accelerating voltage ratio value reduced minimum ion beam divergence. This effect is the opposite of that reported previously for changes to the discharge-to-total accelerating voltage ratio V_D/V_T with two-grid geometries.[2] Uncertainty in the beam floating potential with corresponding net-to-total accelerating voltage ratio uncertainties could be

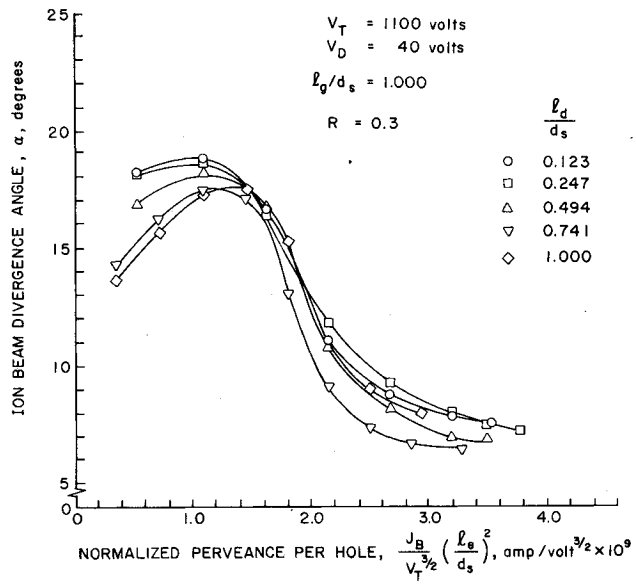

Fig. 6 Effect of l_d/d_s on ion beam divergence (large l_g/d_s and small R).

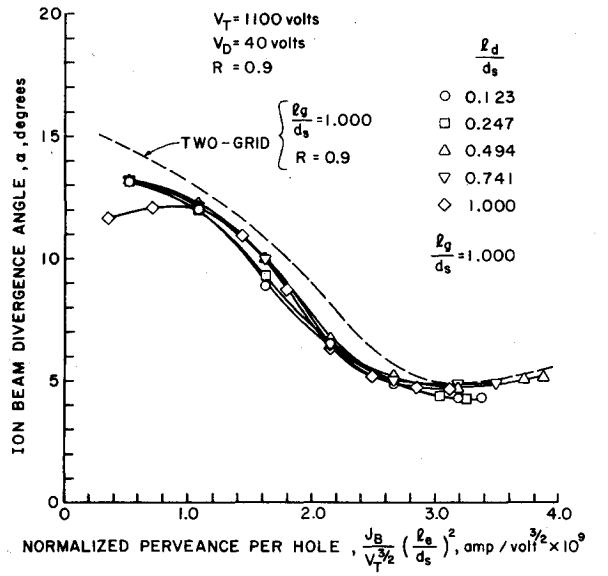

Fig. 7 Effect of l_d/d_s on ion beam divergence (large l_g/d_s and large R).

the cause of this discrepancy. It is possible also that the effect is real, albeit unexplained, and that grid set operation at a few kilovolts total accelerating voltage may produce acceptable ion beam focusing at a net-to-total accelerating voltage ratio of 0.1 over a limited perveance range.

Figures 6 and 7 show the beam divergence characteristics of a low perveance, good focusing grid set as l_d/d_s and R are varied over the range of interest. Comparison of Figs. 6 and 7 shows some striking differences, the most notable being that the minimum beam divergence angle in Fig. 6 occurs not for the minimum l_d/d_s value, as in Fig. 2, but for a rather large l_d/d_s value of about 0.7. There is no obvious reason why this should occur; however, the minimum beam divergence angle variations are small and it is sufficient to note that accelerator-to-decelerator grid separation ratio variations have less effect on the minimum beam divergence angle, at a constant R value, as l_g/d_s is increased. Figure 7 shows the negligible effect l_d/d_s variations have on ion beam divergence for an l_g/d_s value of 1.000 and an R value of 0.9. Only slight focusing gains are evident with the addition of a decelerator grid to a two-grid set which has a large screen-to-accelerator

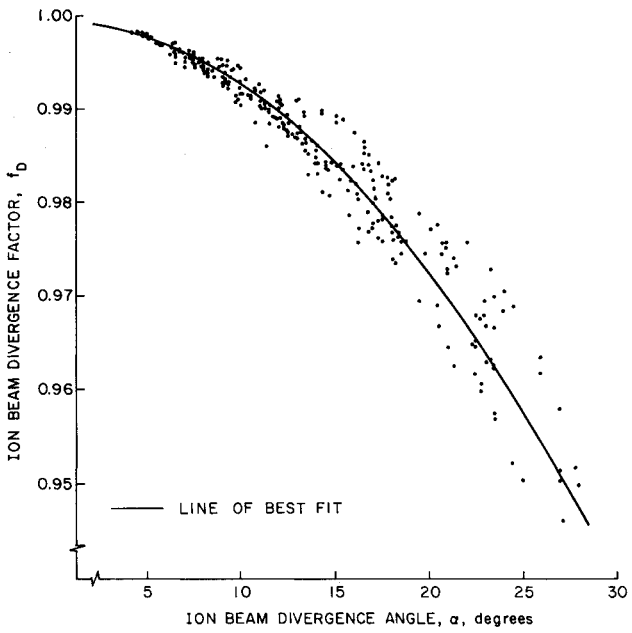

Fig. 8 Ion beam divergence factor f_D as a function of ion beam divergence angle α.

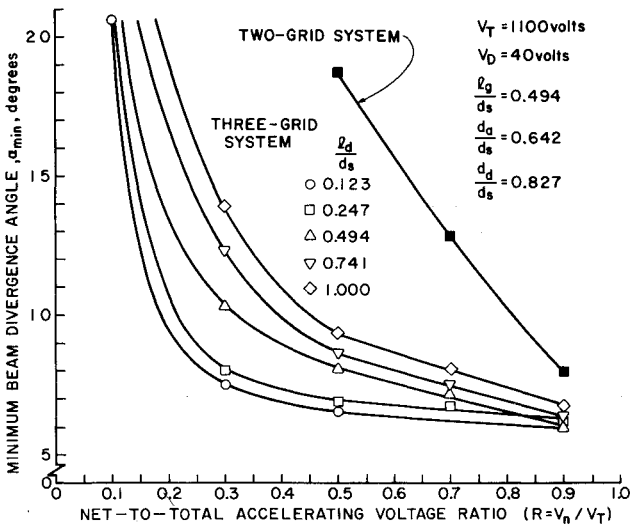

Fig. 9 Effect of the net-to-total accelerating voltage ratio R on the minimum ion beam divergence angle α_{min} for different l_d/d_s values.

grid separation ratio ($l_g/d_s = 1.000$) and is operating at a high net-to-total accelerating voltage ratio ($R = 0.9$). Since neutralizer electron backstreaming limits the maximum net-to-total accelerating voltage ratio to values not much greater than 0.9, one can conclude that l_g/d_s is the most important parameter affecting the absolute minimum beam divergence angle (Figs. 3 and 7)

Figure 8 shows a plot of the ion beam divergence factor f_D as a function of the ion beam divergence angle α. This plot contains results from all of the three-grid accelerator system geometries and operating conditions investigated during this study.[3] The line of best fit drawn in Fig. 8 allows f_D to be estimated once α is known. The magnitude of α may be measured experimentally or may be estimated, based on known grid geometry and operating conditions, from the graphical results contained in this paper and Ref. 3.

Minimum Ion Beam Divergence

Figure 9 is a plot of minimum beam divergence angle α_{min} against R, with l_d/d_s as a parameter. These data were obtained from Figs. 2, 3, and 5 and Ref. 3. A two-grid accelerator system divergence angle curve is shown also in Fig. 9 for comparison. Significant beam divergence angle reductions for three-grid accelerator systems over a two-grid accelerator system are apparent. Spacing the accelerator and decelerator grids as close as possible (lowest l_d/d_s value) gave the lowest minimum beam divergence angles for all values of the net-to-total accelerating voltage ratio. Only two data points were obtained for $R = 0.1$ operation, one is shown for $l_d/d_s = 0.123$ at 20.6 deg while the other is not shown but was for $l_d/d_s = 1.000$ at 28.0 deg. In the latter instance the curve has been faired correctly to meet this point but has been chopped off because of space requirements. The remaining curves, for $l_d/d_s = 0.247$, 0.494, and 0.741, for which no $R = 0.1$ data were obtained, have been interpolated for this region of low net-to-total accelerating voltage ratio. Figure 9 shows that for very low R values the minimum beam divergence angle increases rapidly. However, it should be noted that a rapid increase in the minimum beam divergence angle at very low R values would be expected also for the two-grid system. Extrapolating the two and three-grid minimum divergence angle curves of Fig. 9 shows that they cross at a net-to-total accelerating voltage ratio of about unity. The reduced effectiveness of a three-grid over a two-grid accelerator system, at high net-to-total accelerating voltage ratios, has been pointed out previously by Meadows and Free[1] and Kaufman.[4]

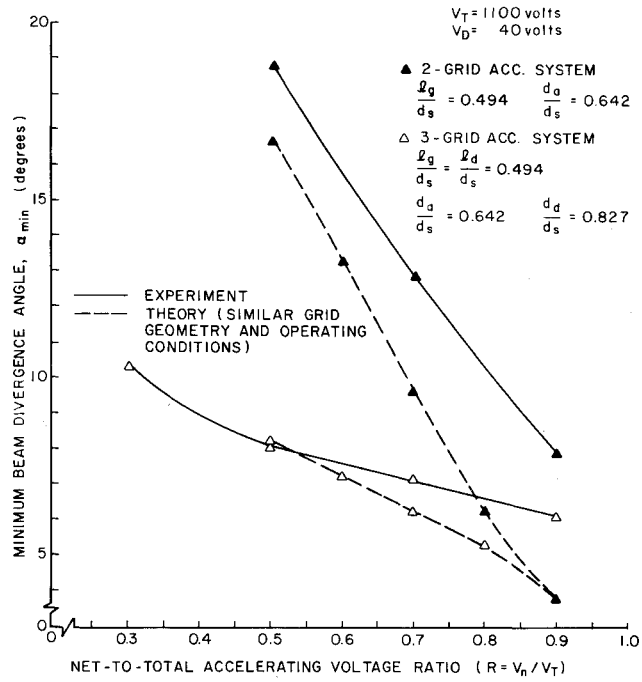

Fig. 10 Comparison of experimental and theoretical α_{min} values fo two- and three-grid accelerator systems.

Figure 10 compares minimum beam divergence angle results obtained experimentally to those obtained theoretically by Kaufman.[4] Qualitative agreement between theory and experiment is good, but the experimental results do show a more substantial reduction in divergence angle associated with the substitution of three for two-grid accelerator systems than theory predicts.

Grid Design

Figure 11 shows the results of tests designed to determine the best d_d/d_s and l_d/d_s for a high perveance grid set (small screen-to-accelerator grid separation ratio l_g/d_s). For these tests, a decelerator hole diameter ratio of $d_d/d_s = 0.827$ and accelerator-to-decelerator grid separation ratio of $l_d/d_s = 0.247$ gave the lowest ion beam divergence. Figure 12 shows that significant decelerator grid impingement occurs as the decelerator hole size approaches the accelerator hole size.

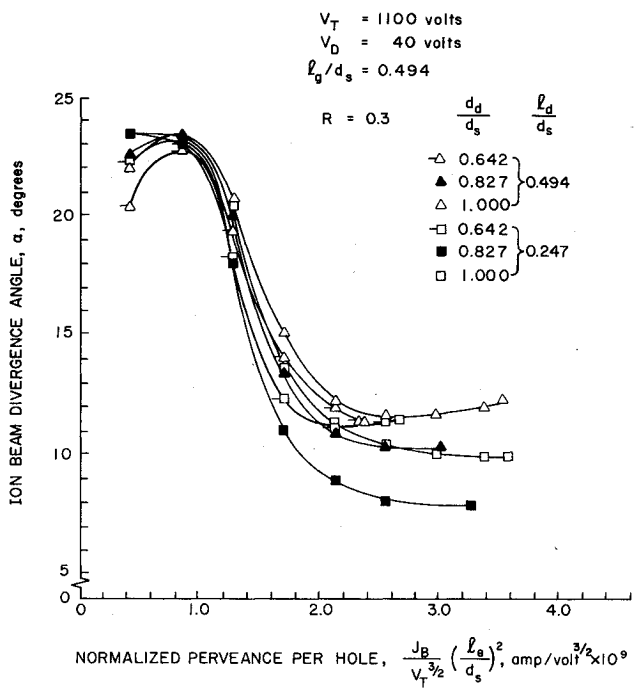

Fig. 11 Effect of d_d/d_s on ion beam divergence (high perveance grid set, small l_g/d_s).

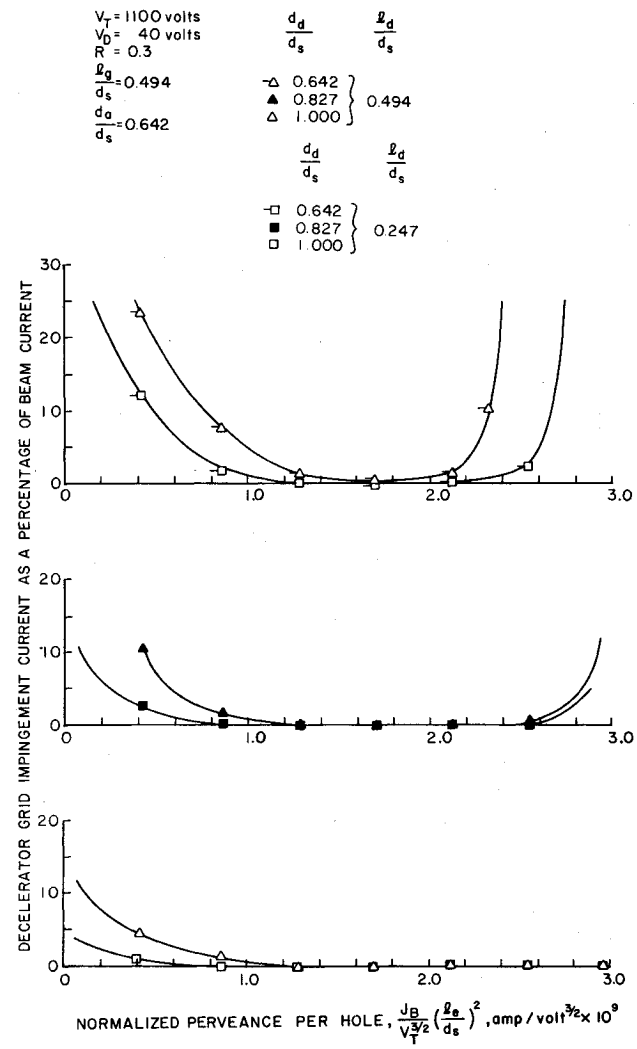

Fig. 12 Effect of d_d/d_s on impingement (high perveance grid set, small l_g/d_s).

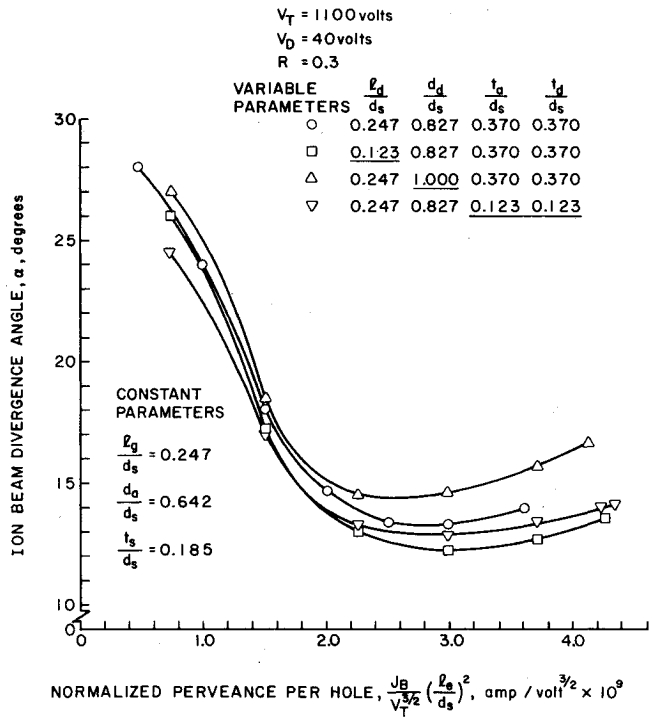

Fig. 13 Effect of d_d/d_s and accelerator (t_a/d_s),and decelerator (t_d/d_s) grid thickness ratios on ion beam divergence (very high perveance grid set, very small l_g/d_s).

For equal accelerator and decelerator hole sizes the decelerator grid impingement current is unacceptably high. It should be noted that small negative decelerator grid impingement currents were observed whenever the beamlet diameter was substantially less than the decelerator hole diameter. This occurs for large decelerator hole diameter ratios, small accelerator-to-decelerator grid separation ratios, and large net-to-total accelerating voltage ratios. These negative decelerator grid impingement currents are thought to be a result of secondary electrons produced by direct ion and charge exchange ion impingement upon the accelerator grid. The secondary electron currents are always present, but they are measurable only when the ion impingement upon the decelerator grid approaches zero. These negative decelerator grid impingement currents were small, being at most 0.2% of the beam current.

Figure 13 shows the results of testing a very high perveance grid set to determine the best d_d/d_s and l_d/d_s. Here, l_g/d_s is 0.247. This represents a screen-to-accelerator grid separation distance of 0.51 mm: about the closest that has been maintained reliably for full size ion thruster accelerator systems. In light of this practical consideration, the superior ion beam focusing shown by reducing the accelerator-to-decelerator grid separation ratio to 0.123 would usually be unrealizable. The best method to decrease ion beam divergence and increase the maximum normalized perveance per hole, given 0.51mm grid spacings, is to have thin accelerator and decelerator grids (inverted triangles in Fig. 13, these grid thicknesses were 0.25 mm). Here again, a d_d/d_s of 0.827 also gave improved focusing. Further tests were done at a net-to-total accelerating voltage ratio of 0.7. The results showed a decrease in the effect accelerator and decelerator grid thickness ratio variations have on the maximum normalized perveance per hole. In summary, Figs. 11-13 indicate that low beam divergence angles and low decelerator grid impingement currents for three grid accelerator systems require that the decelerator hole diameter be about 25% larger than the accelerator hole diameter. This criterion, together with the previously mentioned requirement of spacing the accelerator and decelerator grids as close as is practically possible,

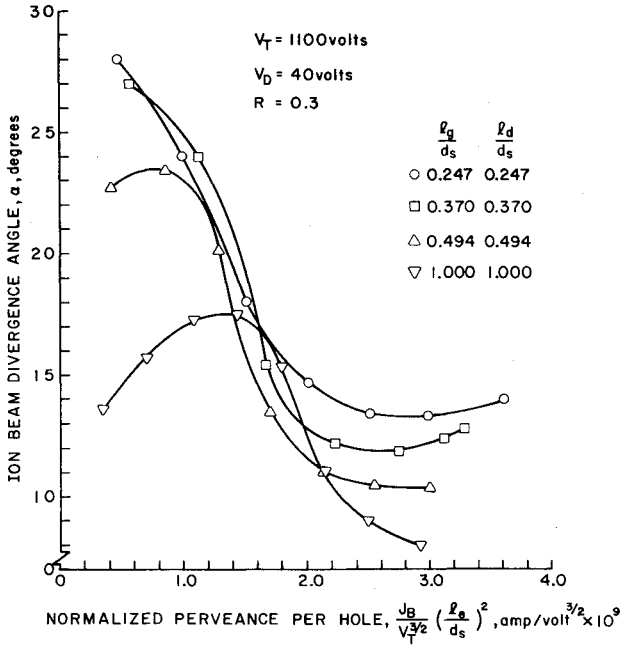

Fig. 14 Effect of l_g/d_s and l_d/d_s grid separation ratios on the minimum ion beam divergence angle operating range.

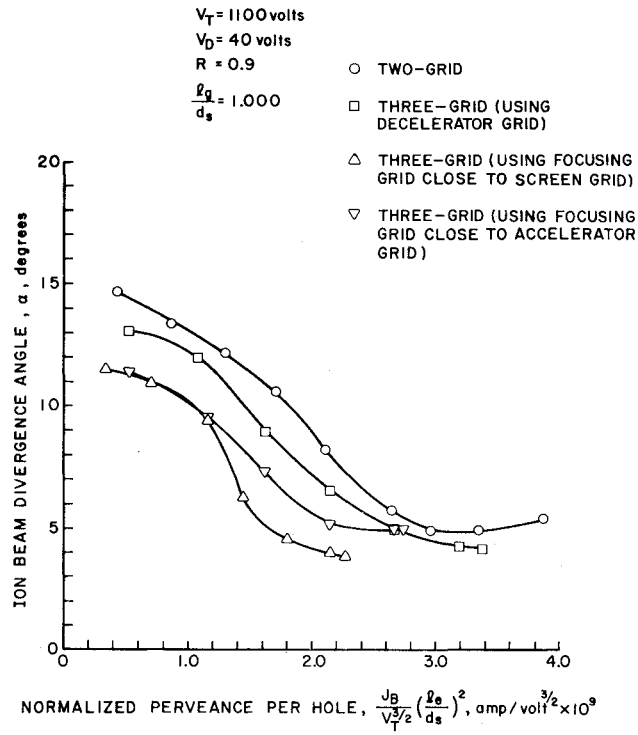

Fig. 15 Effect of two- and three-grid accelerator system configurations on the absolute minimum beam divergence angle (large l_g/d_s and large R).

constitute the major geometric design requirements when considering the use of a decelerator grid.

There is another requirement important to the successful operation of three-grid accelerator systems which has yet not been discussed in detail. This is the operating range of normalized perveance per hole over which the ion beam divergence angle departs only slightly from its minimum value. Figure 14 shows how this operating range decreases with increasing l_g/d_s and l_d/d_s. For the smallest grid separation ratio ($l_g/d_s = l_d/d_s = 0.247$) a broad operating range is evident, while for the largest tested ($l_g/d_s = l_d/d_s = 1.000$) the ion beam divergence angle curve does not reach a minimum. Further increases in the low ion beam divergence angle operating range can be obtained by reducing the accelerator and decelerator grid thickness, as shown previously. Fig. 14 shows that the highest perveance grid sets (smallest screen-to-accelerator and accelerator-to-decelerator grid separation ratios), may be operated over a wide range of normalized perveance per hole values without appreciable ion focusing degradation. In contrast, however, the lower perveance grid sets (larger screen-to-accelerator and accelerator-to-decelerator grid separation ratios) would require close regulation of the ion source beam current to insure continued accelerator system operation over the narrow beam current range at which the minimum beam divergence angle occurs.

Figure 15 shows the results of an effort to obtain the absolute minimum beam divergence angle given an l_g/d_s of 1.000 and an R value of 0.9. The circles in Fig. 14 are for a two-grid accelerator system, while the squares are for a three-grid accelerator system with an l_d/d_s of 0.123. The remaining curves show the effect of placing a third (focusing) grid between the screen and accelerator grid of a two-grid accelerator system. In both cases this focusing grid was biased at, or close to, the Child's law potential one would expect at the focusing grids location if the screen and accelerator grids alone were present. This biasing potential, over the many others tried, gave small minimum beam divergence angles while retaining a reasonable level of beam current. The focusing grid itself had the same hole diameter as the screen grid (2.06 mm) and was 0.25 mm thick. Placing the focusing grid 0.51 mm downstream of the screen grid gave the ion beam divergence angle curve designated by the right-side-up triangles in Fig. 15. Increasing the biasing potential of the focusing grid above the Child's law potential for this configuration allowed the screen hole sheath to move through the screen hole and establish itself just upstream of the focusing grid. This resulted in increased beam divergence and increased beam current, because the effective acceleration length l_e is reduced. Placing the focusing grid 1.02 mm downstream of the screen grid gave the ion beam divergence angle curve designated by the inverted triangles in Fig. 15. Screen hole sheath movement downstream of the screen grid was also observed for this configuration when the focusing grid was biased above the Child's law potential. However, no increase in maximum beam current was observed following this shift, presumably because of the large accelerator grid impingement currents observed after this shift. It should be noted that the limit in normalized perveance per hole, or beam current, for each of the curves shown in Fig. 15 was due to excessive accelerator grid impingement currents. In summary, for low normalized perveance per hole values a focusing grid is beneficial, particularly when positioned close to the screen grid. However, when good focusing, large beam currents and overall accelerator system complexity are considered, a simple two-grid accelerator system is superior. It must be remembered that this conclusion is valid only for $R \geq 0.9$ and $l_g/d_s \geq 1.000$.

Conclusion

The use of three-grid accelerator systems in place of two-grid accelerator systems offers significant improvements in ion beam focusing. These improvements are greatest for low net-to-total accelerating voltage ratios and small screen-to-accelerator grid separation ratios (i.e., high perveance grid sets). Ion beam focusing gains are negligible at a net-to-total accelerating voltage ratio near unity. For a small screen-to-accelerator grid separation ratio, ion beam divergence decreases with decreasing accelerator-to-decelerator grid separation ratios and increasing net-to-total accelerating voltage ratios. This effect becomes small and is masked by second order focusing effects for a large screen-to-accelerator grid separation ratio. Low decelerator grid impingement

currents and low ion beam divergence angles require that the decelerator hole diameter be about 25% larger than the accelerator hole diameter, and that the decelerator grid be spaced as close as is practically possible to the accelerator grid. These criteria constitute the major geometric design requirements when considering the use of a decelerator grid.

The absolute minimum ion beam divergence angle depends only on the screen-to-accelerator grid separation ratio, provided values of this parameter are at least 1.0 and the net-to-total accelerating voltage ratio is near the electron backstreaming limit. Under these conditions, the addition of a third grid, either as a decelerator grid or as a focusing grid positioned between the sceen and accelerator grids, does not reduce appreciably the absolute minimum beam divergence angle obtained by using a two-grid accelerator system.

Acknowledgment

This research was supported by NASA under Grant NGR-06-002-112.

References

[1]Meadows, G. A. and Free, B. A.,"Effect of a Decel Electrode on Primary and Charge-Exchange Ion Trajectories," AIAA Paper 75-427, 1975.

[2]Aston, G., Kaufman, H. R., and Wilbur, P. J., "Ion Beam Divergence Characteristics of Two-Grid Accelerator Systems," *AIAA Journal,* Vol. 16, May 1978, pp. 516-524.

[3]Aston, G. and Kaufman, H. R., "Ion Beam Divergence Characteristics of Three-Grid Accelerator Systems," AIAA Paper 78-669, San Diego, Calif., April 1978.

[4]Kaufman, H. R., "Accelerator System Solutions for Broad-Beam Ion Sources," *AIAA Journal,* Vol. 15, July 1977, pp. 1025-34.